

1 Ergodicity test of the eddy-covariance technique

2 Jinbei CHEN¹ Yinqiao HU² Ye YU Shihua LÜ

3 *Key Laboratory of Land Surface Processes and Climate Change in Cold and Arid Regions; Cold and*
4 *Arid Regions Environment and Engineering Institute, Chinese Academy of Sciences, Lanzhou 730000, P*
5 *R China.*

6 *Pingliang Land Surface Process & Severe Weather Research Station, Chinese Academy of Science,*
7 *Pingliang 744015, P R China.*

8 1 E-mail: chenjinbei@lzb.ac.cn

9 2 Corresponding author: hyq@ns.lzb.ac.cn

10

11 Abstract

12 The ergodic hypothesis is a basic hypothesis typically invoked in atmospheric surface
13 layer (ASL) experiments. The ergodic theorem of stationary random processes is
14 introduced to analyze and verify the ergodicity of atmospheric turbulence measured
15 using the eddy-covariance technique with two sets of field observational data. The
16 results show that the ergodicity of atmospheric turbulence in ABL is not only relative
17 to the atmospheric stratification but also to the eddy scale of atmospheric turbulence.
18 The eddies of atmospheric turbulence, of which the scale is smaller than the scale of
19 the atmospheric boundary layer (ABL), i.e., the spatial scale is less than 1,000 m and
20 temporal scale is shorter than 10 min, effectively satisfy the ergodic theorems. Under
21 these restrictions, a finite time average can be used as a substitute for the ensemble
22 average of atmospheric turbulence. Whereas, eddies that are larger than ABL scale
23 dissatisfy the mean ergodic theorem. Consequently, when a finite time average is used
24 to substitute for the ensemble average, the eddy-covariance technique incurs large
25 errors due to the loss of low frequency information associated with larger eddies. A
26 multi-stations observation is compared with a single-station, and then the scope that
27 satisfies the ergodic theorem is extended from scales smaller than the ABL
28 approximately 1000 m to scales greater than that about 2000 m. Therefore, the
29 calculation results of averages, variances and fluxes of turbulence are more faithfully
30 approximate the actual values due to effectively satisfy the ergodic assumption.
31 Regardless of vertical velocity or temperature, the variance of eddies at different
32 scales follows Monin-Obukhov Similarity Theory (MOST) better if the ergodic
33 theorem can be satisfied, if not it deviates from MOST. The exploration of ergodicity
34 in atmospheric turbulence is doubtlessly helpful in understanding the issues in

35 atmospheric turbulent observations, and provides a theoretical basis for overcoming
36 related difficulties.

37 **Keywords:** Ergodic hypothesis; eddy-covariance technique; Monin-Obukhov
38 similarity theory (MOST); atmospheric surface layer (ASL); high-pass filtering

39 **1 Introduction**

40 The basic principle of average of the turbulence measurements is based on ensembles
41 averaged over space, time and state. However, it is impossible to make an actual
42 turbulence measurement with enough observational instruments in space for sufficient
43 time to obtain all states of turbulent eddies to achieve the goal of an ensemble average.
44 Therefore, based on the ergodic hypothesis, the time average of one spatial point,
45 taken over a sufficiently long observational time, is used as a substitute for the
46 ensemble average for temporally steady and spatially homogeneous surfaces (Stull
47 1988; Wyngaard 2010; Aubinet 2012). The ergodic hypothesis is a basic assumption
48 in turbulence experiments in the atmospheric boundary layer (ABL) and atmospheric
49 surface layer (ASL). Stationarity, homogeneity, and ergodicity are routinely used to
50 link ensemble statistics (mean and higher-order moments) of field experiments in the
51 ABL. Many authors habitually refer to the ergodicity assumption with descriptions
52 such as “when satisfying ergodic hypothesis.....” or “something indicates that
53 ergodic hypothesis is satisfied”. The success of Monin-Obukhov Similarity Theory
54 (MOST) for unstable and near-neutral conditions is just evidence of the validity of the
55 ergodic hypothesis in the ASL. While ergodicity is a necessary condition for the
56 success of MOST, it does not prove ergodicity (Katul et al. 2004). The success of
57 MOST under the conditions of stationary and homogeneity implies that the stationary
58 and homogeneity are also the important conditions of ASL ergodicity. Therefore,
59 many ABL experiments focus on seeking ideal homogeneous surfaces. Some test
60 procedures are widely applied to establish stationarity (Foken and Wichura 1996;
61 Vickers and Mahrt 1997). Katul and Hsieh (1999) qualitatively analyzed the
62 ergodicity problem in atmospheric turbulence, and believed that it is common for the
63 neutral and unstable ASL to satisfy ergodicity, while it is difficult to reach ergodicity
64 in the stable ASL. Eichinger et al. (2001) indicate that LIDAR (Light Detection and
65 Ranging) technique opens up new possibilities for atmospheric measurements and
66 analyses by providing spatial and temporal atmospheric information with

68 simultaneous high-resolution. The stationarity and ergodicity can be tested for such
69 ensembles of experiments. Recent advance in LIDAR measurements offers a
70 promising first step for direct evaluation of such hypotheses for ASL flows (Higgins
71 et al., 2013). Higgins et al. (2013) applied LIDAR of water vapor concentration to
72 investigate the ergodic hypothesis of atmospheric turbulence for the first time. It is
73 clear all the same that there is a need to reevaluate the technologies of turbulence
74 measurement, to test the ergodicity of atmospheric turbulence quantitatively by means
75 of observation experiments.

76 The ergodic hypothesis was first proposed by Boltzmann (Boltzmann 1871; Uffink
77 2004) in his study of the ensemble theory of statistical dynamics. He argued that a
78 trajectory traverses *all* points on the energy hypersurface after a certain amount of
79 time. At the beginning of 20th century, the Ehrenfest couple (Ehrenfest. and
80 Ehrenfest-Afanassjewa 1912; Uffink 2004) proposed a quasi-ergodic hypothesis and
81 changed the term “traverses *all* points” in the aforesaid ergodic hypothesis to “passes
82 arbitrarily close to every point”. The basic points of ergodic hypothesis or
83 quasi-ergodic hypothesis recognize that the macroscopic property of a system in the
84 equilibrium state is an average of microcosmic quantity in sufficient long time.
85 Nevertheless, the ergodic hypothesis or quasi-ergodic hypothesis were never proven
86 theoretically. The proof of the ergodic hypothesis in physics aroused the interest of
87 mathematicians. Famous mathematician, Neumann et al. (1932) first theoretically
88 proved the ergodic theorem in topological space (Birkhoff 1931, Krengel 1985).
89 Afterward, a banausic ergodic theorem of stationary random processes was proved to
90 provide a necessary and sufficient condition for the ergodicity of stationary random
91 processes. Mattingly (2003) reviewed the research progress on ergodicity for
92 stochastically force Navier-Stokes equation, and that Galanti and Tsinober (2004) and
93 Lennaert et al. (2006) solved the Navier-Stokes equation by numerical simulation to
94 prove that turbulence that is temporally steady and spatially homogeneous is ergodic.
95 However, Galanti and Tsinober (2004) also indicated that such partially turbulent
96 flows acting as mixed layer, wake flow, jet flow, flow around the boundary layer may
97 be non-ergodic.

98 Obviously, the advances of research on ergodicity in the mathematics and physics
99 have led the way for the atmospheric sciences. We try first to introduce the ergodic
100 theorem of stationary random processes to the atmospheric turbulence in this paper.

101 The ergodicity of different scale eddies of atmospheric turbulence is directly analyzed
102 and verified quantitatively on the basis of field observation data obtained using
103 eddy-covariance technique in the ASL.

104 **2 Theories and methods**

105 **2.1 Ergodic theorems of stationary random processes**

106 Stationary random processes are processes which will not vary with time, i.e., for
107 observed quantity A , its function of space x_i and time t_i satisfies the following
108 condition:

109
$$A(x_1, x_2, \dots, x_n; t_1, t_2, \dots, t_n) = A(x_1, x_2, \dots, x_n; t_1 + \tau, t_2 + \tau, \dots, t_n + \tau), \quad (1)$$

110 where τ is a time period, defined as the relaxation time.

111 The mean μ_A of a random variable A and its autocorrelation function $R_A(\tau)$ are
112 respectively defined as following:

113
$$\mu_A = \lim_{T \rightarrow +\infty} \frac{1}{T} \int_0^T A(t) dt, \quad (2)$$

114
$$R_A(\tau) = \lim_{T \rightarrow +\infty} \frac{1}{T} \int_0^T A(t) A(t + \tau) dt. \quad (3)$$

115 The autocorrelation function $R_A(\tau)$ is a temporal second-order moment. In the case of
116 $\tau=0$, the autocorrelation function $R_A(\tau)$ is the variance of random variable. A necessary
117 and sufficient condition for the stationary random processes to satisfy the mean
118 ergodicity is the mean ergodic function $Ero(A)$ to zero (Papoulis and Pillai 1991), as
119 shown below:

120
$$Ero(A) = \lim_{T \rightarrow \infty} \frac{1}{T} \int_0^{2T} \left(1 - \frac{\tau}{2T} \right) [R_A(\tau) - \mu_A^2] d\tau = 0. \quad (4)$$

121 The mean ergodic function $Ero(A)$ is a time integral of the difference between the
122 autocorrelation function $R_A(\tau)$ of variable A and its mean square, μ_A^2 . If the mean
123 ergodic function $Ero(A)$ converges to zero, then the stationary random processes will
124 be ergodic. In other words, if the autocorrelation function $R_A(\tau)$ of variable A
125 converges to its mean square, μ_A^2 , the stationary random processes are mean ergodic.
126 The Eq. (4) is namely mean ergodic theorem to be called as well as ergodic theorem
127 of the *weakly* stationary processes in the mathematics. For discrete variables, Eq. (4)
128 can be rewritten as following:

129
$$\text{Ero}(A) = \lim_{n \rightarrow \infty} \sum_{i=0}^n \left(1 - \frac{\tau_i}{n}\right) \left[R_A(\tau_i) - \mu_A^2 \right] = 0. \quad (5)$$

130 Eq. (5) is mean ergodic theorem of the discrete variable. Hence, Eq. (4) or (5) can be
131 used as a criterion to judge the mean ergodicity.

132 For the stationary random processes, the necessary and sufficient condition
133 satisfying the autocorrelation ergodicity is the autocorrelation ergodic function $\text{Er}(A)$
134 to zero:

135
$$\text{Er}(A) = \lim_{T \rightarrow \infty} \frac{1}{T} \int_0^{2T} \left(1 - \frac{\tau'}{2T}\right) \left[B(\tau') - |R_A(\tau)|^2 \right] d\tau' = 0; \quad (6a)$$

136
$$B(\tau') = E \left\{ A(t + \tau + \tau') A(t + \tau') \left[A(t + \tau) A(t) \right] \right\}. \quad (6b)$$

137 Where τ' is a differential variable for entire relaxation times, and that $B(\tau')$ is temporal
138 fourth-order moment of variable A . The autocorrelation ergodic function $\text{Er}(A)$ is a
139 time integral of the difference between the temporal fourth-order moment $B(\tau')$ of
140 variable A and its autocorrelation function square, $|R_A(\tau)|^2$. If the autocorrelation
141 ergodic function $\text{Er}(A)$ converges to zero, then the stationary random processes will be
142 of autocorrelation ergodicity, and thus the autocorrelation ergodicity means that the
143 fourth-order moment of variable of stationary random processes will converge to
144 square of its autocorrelation function $R_A(\tau)$. Eq. (6a) is namely autocorrelation ergodic
145 theorem to be called as well as ergodic theorem of the *strongly* stationary processes in
146 the mathematics. The autocorrelation ergodic function of corresponding discrete
147 variable can be determined as following:

148
$$\text{Er}(A) = \lim_{n \rightarrow \infty} \sum_{i=0}^n \left(1 - \frac{\tau'_i}{n}\right) \left[B(\tau'_i) - |R_A(\tau_j)|^2 \right] = 0, \quad (7a)$$

149
$$B(\tau'_{i,j}) = E \left\{ \sum_{j=0}^n A(t + \tau_j + \tau'_{i,j}) A(t + \tau'_{i,j}) \left[A(t + \tau_j) A(t) \right] \right\}. \quad (7b)$$

150 Eq. (7a) is autocorrelation ergodic theorem of the discrete variable. Hence, Eq. (6a) or
151 (7a) can also be used as a criterion to judge the autocorrelation ergodicity.

152 The stationary random processes conform to the criterion, Eq. (4) or (5), then they
153 satisfy the mean ergodic theorem, or are intituled as the mean ergodicity; the
154 stationary random processes conform to the criterion, Eq. (6a) or (7a), then they
155 satisfy the autocorrelation ergodic theorem, or are intituled as the autocorrelation

156 ergodicity. If the stationary random processes are only of mean ergodicity, they are
157 strict ergodic or narrow ergodic. If the stationary random processes are of both the
158 mean ergodicity and autocorrelation ergodicity, they are namely wide ergodic
159 stationary random processes. It is thus clear that the ergodic random processes are
160 stationary, but the stationary processes may not be ergodic.

161 In the random process theory, calculating the mean or high-order moment function
162 requires a large amount of repeated observations to acquire a sample function $A_k(t)$. If
163 the stationary random processes satisfy the ergodic condition, then time average of a
164 sample on the whole time shaft can be used to substitute for the ensemble average.
165 Eqs. (4), (5), (6a) and (7a) can be used as the criterion to judge whether or not
166 satisfying the mean and autocorrelation ergodicity. The ergodic random processes
167 must be the stationary random processes to be defined as Eq. (1), and thus are
168 stationary in relaxation time τ . If the condition such as Eq. (4) or (5) of the mean
169 ergodicity is satisfied, then a time average in finite relaxation time τ can be used to
170 substitute for infinite time average to calculate the mean Eq. (2) of random variable;
171 similarly, the finite time average can be used for substitution to calculate the
172 covariance or variance of random variable, Eq. (3), if the condition such as Eq. (6a) or
173 (7a) of autocorrelation ergodicity is satisfied. In a similar manner, the basic principle
174 of average of the atmospheric turbulence is the ensemble average of space, time and
175 state, and it is necessary to carry through mass observations for a long period of time
176 in the whole space. This is not only a costly observation, even is hardly feasible. If the
177 turbulence satisfies the ergodic condition, then a time average in relaxation time τ by
178 multi-stations observation, even single-station observation, can substitute for the
179 ensemble average. In fact, precondition to estimate turbulent characteristic quantities
180 and fluxes in the ABL by the eddy-covariance technique is that the turbulence satisfies
181 the ergodic condition. Therefore, conditions such as Eqs. (4), (5), (6a) and (7a) will
182 also be the criterion for testing the authenticity of results observed by the
183 eddy-covariance technique.

184 **2.2 Band-pass filtering**

185 The scope of spatial and temporal scale of the atmospheric turbulence, which is from
186 the dissipation range, inertial sub-range to the energy range, and further the turbulent
187 large eddy, is extremely broad (Stull 1988). In such wide spatial and temporal scope,
188 the turbulent eddies include the isotropic 3-D eddy structure of high frequency

189 turbulence and orderly coherent structure of low frequency turbulence (Li et al. 2002).
 190 These eddies of different scale are also each other different in terms of their spatial
 191 structure and physical properties, and even their transport characteristics are not all
 192 same. It is thus reasonable that eddies with different characteristics are separated,
 193 processed and studied using different methods (Zuo et al. 2012). A major goal of our
 194 study is to understand what type of eddy in the scale can satisfy the ergodic condition.
 195 Another goal is that the time averaging of signals measured by a single station
 196 determines accurately turbulent characteristic quantities. In order to study the
 197 ergodicity of different scale eddies, Fourier transform is used as a band-pass filtering
 198 to distinguish different scale eddy. That is to say, we set the Fourier transform
 199 coefficient of the part of frequencies, which does not need, as zero, and then acquire
 200 the signals after filtering by means of Fourier inverse transformation. The specific
 201 formulae are shown below:

$$202 \quad F_A(n) = \frac{1}{N} \sum_{k=0}^{N-1} A(k) \cos\left(\frac{2\pi nk}{N}\right) - \frac{i}{N} \sum_{k=0}^{N-1} A(k) \sin\left(\frac{2\pi nk}{N}\right), \quad (8)$$

$$203 \quad A(k) = \sum_{n=a}^{N-1} F_A(n) \cos\left(\frac{2\pi nk}{N}\right) + i^2 \sum_{n=a}^{N-1} F_A(n) \sin\left(\frac{2\pi nk}{N}\right). \quad (9)$$

204 In Eqs. (8) and (9), $F_A(n)$ and $A(k)$ are respectively the Fourier transformation and
 205 Fourier inverse transformation including N data points from $k=0$ to $k=N-1$, and n is the
 206 cycle index of the observation time range. The high-pass filtering can cut off the low
 207 frequency signals of turbulence to obtain the high frequency signals. An aliasing of
 208 half high frequency turbulence after the Fourier transformation is unavoidable. At this
 209 time, the correction for high frequency response will compensate for that loss. In
 210 order to acquire purely signals of different scale eddies in filtering processes, we take
 211 results of the band-pass filtering from $n=j$ to $n=N-j$ as required signals. This is referred
 212 to as j time filtering in this paper. Finally, the ergodicity of different scale eddies is
 213 analyzed using Eqs. (4)-(7).

214 2.3 MOS of turbulent variance

215 The characteristics of the relations of Monin-Obukhov Similarity (MOS) for the
 216 variance of different scale eddies are analyzed and compared to test feasibility of the
 217 MOS relation for ergodic and non-ergodic turbulence. In order to provide an
 218 experimental basis for utilizing MOST and developing the turbulence theory of ABL
 219 under the condition of the complex underlying surfaces, the problems of

220 eddy-covariance technique of the turbulence observation in ASL are further explored
 221 on the basis of studying on the ergodicity and MOS relations of the variance of
 222 different scale eddies.

223 The MOS relations of turbulent variance can be regarded as an effective
 224 instrumentality to verify whether or not that the turbulent flow field is steady and
 225 homogeneous (Foken et al. 2004). Under ideal conditions, the local MOS relations of
 226 the variance of wind velocity, temperature and other factors can be expressed as
 227 following:

$$228 \quad \sigma_i / u_* = \phi_i(z/L), \quad (i = u, v, w), \quad (10)$$

$$229 \quad \sigma_s / |s_*| = \phi_s(z/L), \quad (s = \theta, q). \quad (11)$$

230 where σ is turbulent variance; corner mark i is wind velocity u , v or w ; s stands for
 231 scalar, such as potential temperature θ and humidity q ; u_* is friction velocity and
 232 defined as $u_* = (\overline{u'w'}^2 + \overline{v'w'}^2)^{1/4}$; s_* is turbulent characteristic quantity related to
 233 scalar defined as $s_* = -\overline{w's'}/u_*$; and that M-O length L is defined as (Hill 1989):

$$234 \quad L = u_*^2 \theta / [\kappa g(\theta_* + 0.61 \theta q_*/\rho_d)], \quad (12)$$

235 where ρ_d is dry air density .

236 A large number of research results show that, in the case of unstable stratification,
 237 $\phi_i(z/L)$ and $\phi_s(z/L)$ can be expressed in the following forms (Panofsky et al. 1977;
 238 Padro 1993; Katul et al. 1999):

$$239 \quad \phi_i(z/L) = c_1 (1 - c_2 z/L)^{1/3}; \quad (13)$$

$$240 \quad \phi_s(z/L) = \alpha_s (1 - \beta_s z/L)^{-1/3}. \quad (14)$$

241 where c_1 , c_2 , α and β are coefficient to be determined by the field observation. In the
 242 case of stable stratification, $\phi_s(z/L)$ approximates a constant and $\phi_i(z/L)$ is still the
 243 $1/3$ function of z/L . The turbulent characteristics of eddies in different temporal and
 244 spatial scale are analyzed and compared with the mean and autocorrelation ergodic
 245 theorems, to test feasibility of MOS relations under the condition of the ergodic and
 246 non-ergodic turbulence.

247 **3 The sources and processing of data**

248 In this study two turbulence data sets are used for completely different purposes. The
249 first turbulence data set is the data measured by the eddy-covariance technique under
250 the homogeneous surface in Nagqu Station of Plateau Climate and Environment
251 (NSPCE), Chinese Academy of Sciences (CAS). The data set in NSPCE/CAS
252 includes the data that are measured by 3-D sonic anemometer and thermometer
253 (CSAT3) with 10 Hz as well as infrared gas analyzer (Li7500) in ASL from 23 July to
254 13 September 2011. In addition, the second turbulence data set of CASES-99 (Poulos
255 et al. 2002; Chang and Huynh. 2002) is used to verify the ergodicity of turbulence
256 observed by multi-stations. CASES-99 has seven observation sites to be equivalent to
257 seven observation stations. The data in the central tower of CASES-99 include that
258 measured by sonic anemometer and thermometer (CSAT3) with 20 Hz and the
259 infrared gas analyzer (Li7500) at 10m on tower with 55 m height in ASL. The other
260 six sub-sites of CASES-99 surrounding the central tower, sn1, sn2 and sn3 are located
261 100 m are away from the central tower, the sub-site sn4 is 280 m away, and sub-sites
262 sn5 and sn6 are located 300 m away. The data of sub-sites include that measured by
263 3-D sonic anemometer (ATI) and Li7500 at 10 m height on the towers. The analyzed
264 results with two data sets are compared each other to test universality of the research
265 results.

266 The geographic coordinate of NSPCE/CAS is 31.37°N, 91.90°E, and its altitude is
267 4509 m a.s.l. The observation station is built on flat and wide area except for a hill of
268 about 200 m at 2 km distance in the north, and floor area is 8000m². The ground
269 surface is mainly composed of sandy soil mixed with sparse fine stones, and a plateau
270 meadow with vegetation of 10-20 cm. The roughness length and displacement height
271 of underlying surface of NSPCE meadow are respectively 0.009 m and 0.03 m.
272 CASES-99 is located in prairie of Kansas US. The geographic coordinate of
273 CASES-99 central tower is 37.65°N, 96.74°W. The observation field is flat and
274 growth grasses about 20-50 cm during the observation period, while the roughness
275 length and displacement height of CASES-99 underlying surface are 0.012 m and
276 0.06 m, respectively (Martano 2000).

277 These data are used to study the ergodicity of turbulent eddies in ABL. Firstly the
278 inaccurate data caused by spike are deleted before data analyses. Subsequently, the
279 data are divided into continuous sections of 5-hour, and the signals of 1-hour are
280 obtained applying filtering of Eqs. (8) and (9) for each 5-hour data. In order to delete

281 further the abnormal inaccurate data, the data are divided once again into 12
282 continuous fragments of 5-min in 1-hour. The variances of velocity and temperature
283 are calculated and compared each other for the fragments. The data that deviation is
284 less than $\pm 15\%$ including an instrumental error about $\pm 5\%$ are selected to use.
285 Moreover, temperature of the ultrasonic pulse signals is converted to the absolute
286 temperature (Schotanus et al. 1983; Kaimal and Gaynor 1991). Then all data without
287 spike for 25 days are done the coordinate rotation using the plane fitting method to
288 improve the levelness of instrument installation (Wilczak 2001). The trend correction
289 (McMillen 1988; Moore 1986) is used to exclude the influence of low-frequency
290 trend effect caused by the diurnal variations and weather processes. The Webb
291 correction (Webb et al. 1980) is a component of surface energy balance in physical
292 nature, but not the component of turbulent eddy. However, this study is to analyze the
293 ergodicity of turbulent eddies. According to our preliminary analysis about the
294 ergodicity of turbulent eddies, such correction may cause the unreasonable deviation
295 from the prediction with Eq. (14). We thus do not perform the Webb correction in our
296 research on the ergodicity.

297 **4. Result analyses**

298 Applying the two data sets from NSPCE/CAS and CASES-99, the ergodicity of
299 different temporal scale eddies is tested. Here as an example, we select representative
300 data measured at level of 3.08m in NSPCE/CAS during three time frames, namely
301 3:00-4:00, 7:00-8:00 and 13:00-14:00 China Standard Time (CST) on 25 August in
302 clear weather to test and demonstrate the ergodicity of different temporal scale eddies.
303 These three time frames represent three situations, i.e. the nocturnal stable boundary
304 layer, early neutral boundary layer and midday convective boundary layer.

305 Eqs. (8) and (9) are used to perform band-pass filtering from $n=j$ to $n=N-j$ to
306 acquire the signals of eddies corresponding temporal scale including 2 min, 3 min, 5
307 min, 10 min, 30 min and 60 min. The turbulence characteristics and ergodicity of
308 eddies in the different temporal scale including 2 min, 3 min, 5 min, 10 min, 30 min
309 and 60 min are studied using above processed data for three time frames.

310 **4.1 M-O eddy local stability and M-O stratification stability**

311 The M-O stratification stability parameter z/L describes a whole characteristic of the
312 mechanical and buoyancy effect on the ASL turbulence. However this study will
313 decompose the turbulence into different scale eddies. Considering that the property of

314 different scale eddies of the atmospheric turbulence varies with the atmospheric
315 stability parameter z/L , a M-O eddy local stability that is limited in the certain scale
316 range of eddies is defined as z/L_c , so as to analyze relations between the stratification
317 stability and ergodicity of the different scale eddies for the wind velocity, temperature
318 and other factors. It is worth noting that the M-O eddy local stability, z/L_c , is different
319 from the M-O stratification stability, z/L .

320 As a typical example, the eddy local stabilities, z/L_c , of the different temporal scales
321 for the three time frames from the nighttime to the daytime are shown in Table 1. The
322 results show that the eddy local stability z/L_c below 2 min in temporal scale at time
323 3:00-4:00 AM (CST) during the nighttime time frame is 0.59, thus it is stable
324 stratification. But as the eddy temporal scale gradually increases from 3 min, 5 min
325 and 10 min to 60 min, the eddy local stability, z/L_c , gradually decreases to 0.31 and
326 0.28. Even starting from 10 min in the temporal scale, the eddy local stability
327 decreases from -0.01 to -0.07. It seems that the eddy local stability gradually varies
328 from stable to unstable as the eddy temporal scale increases. At 7:00-8:00 AM (CST)
329 during the morning time frame, the eddy local stability z/L_c from 2 min to 60 min in
330 the temporal scale eventually decreases from 0.52, 0.38, 0.16 and 0.15 to -0.43 in 30
331 min and a minimum of -1.29 in 60 min. It means that eddies in the temporal scales of
332 30 min and 60 min have high local instability. However, at 14:00-15:00 PM (CST)
333 during the midday time frame, eddies in the temporal scales from 2 min to 60 min are
334 all unstable. Now $-z/L_c$ is defined as eddy local instability. As the eddy scale increases,
335 the eddy local instability in the scales from 2 min to 3 min also increases. And that its
336 value reaches a maximum of 0.44 as the eddy scale is at 5 min. But as the eddy scale
337 increases continuously, the eddy local instability is reduced.

338 The M-O eddy local stability is not entirely the same as the M-O stratification
339 stability of ABL in the physical significance. The M-O stratification stability of ABL
340 indicates the overall effect of atmospheric stratification in the ABL on the stability
341 including all eddies in integral boundary layer. The M-O stratification stability z/L is
342 stable 0.02 at 3:00-4:00 AM (CST) for no filtering data to include whole turbulent
343 signals, but unstable -0.004 and -0.54 at 7:00-8:00 and 13:00-14:00 PM (CST),
344 respectively. However the eddy local stability is only a local effect of atmospheric
345 stratification on the stability of eddies in a certain scale. As the eddy scale increases,
346 the eddy local stability z/L_c will vary accordingly. The aforesaid results indicate that

347 the local stability of small-scale eddies is stable in the nocturnal stable boundary layer,
348 but it is possibly unstable for the large-scale eddies. As a result, a sink effect on the
349 small-scale eddies in the nocturnal stable boundary layer, but a positive buoyancy
350 effect on the large-scale eddies. However, in diurnal unstable boundary layer, the eddy
351 local instability of 3 min scale reaches a maximum, and then the instability gradually
352 decreases as the eddy scale increases. Therefore, eddies of 3 min scale hold maximum
353 buoyancy, but the eddy buoyancy decreases as the eddy scale increases continuously.
354 Nevertheless, the small-scale eddies are more stable than the large scale eddies in the
355 nocturnal stable boundary layer; the large-scale eddies are more stable than the small
356 scale eddies in the diurnal convective boundary layer with unstable stratification. The
357 above facts signify that it is common that there exist mainly the small-scale eddies in
358 the nocturnal boundary layer with stable stratification. And it is also common that
359 there exist mainly the large-scale eddies in the diurnal convective boundary layer with
360 unstable stratification. Therefore, it can well understand that the small-scale eddies are
361 dominant in the nocturnal stable boundary layer, while the large-scale eddies are
362 dominant in the diurnal convective boundary layer.

363 **4.2 Verification of mean ergodic theorem of eddies in different temporal scale**

364 In order to verify the mean ergodic theorem, we calculate the mean and
365 autocorrelation functions using Eq. (2) and Eq. (3), then calculate the variation of
366 mean ergodic function $Ero(A)$ using Eq. (5) of eddies in the different temporal scale
367 with relaxation time τ to be cut off with $\tau_{i=n}$. The mean ergodic functions, $Ero(A)$, of
368 vertical velocity, temperature and specific humidity of the different scale eddies are
369 calculated using data at level of 3.08m at 3:00-4:00, 7:00-8:00 and 13:00-14:00 (CST)
370 for three time frames in NSPCE/CAS, as shown in Figs. 1-3 respectively. Since the
371 ergodic function varies within a large range, the ergodic functions are normalized
372 according to the characteristic quantity of relevant variables ($A_* = \mathbf{u}_*, |\theta_*|, |q_*|$). That is
373 to say, functions in all following figures are the dimensionless ergodic functions,
374 $Ero(A)/A_*$.

375 Comprehensive analyses of the characteristics of mean ergodicity of atmospheric
376 turbulence as well as the relevant causes:

377 **4.2.1 Verifying mean ergodic theorem of different scale eddies**

378 According to the mean ergodic theorem, Eq. (4), the mean ergodic function $Ero(A)/A_*$
379 will converge to 0 if the time approaches infinite. This is only a theoretical result of

380 the stationary random processes. A practical mean ergodic function is calculated under
381 the condition of that relaxation time $\tau_{i=n}$ is cut off. If the mean ergodic function
382 $Ero(A)/A^*$ converges approximately to 0 in relaxation time $\tau_{i=n}$, it will be considered
383 that random variable A approximately satisfies the mean ergodic theorem. The mean
384 ergodic function deviates more from zero, the mean ergodicity will be of poor quality.
385 Consequently, we can judge approximately the mean ergodic theorem of different
386 scale eddies whether or not holds. Figs. 1-3 clearly show that, regardless of the
387 vertical velocity, temperature or humidity, the $Ero(A)/A^*$ of eddies below 10 min in the
388 temporal scale will swing around zero within a small range; thus we can conclude that
389 the mean ergodic function $Ero(A)/A^*$ of eddies below 10 min in the temporal scale
390 converges to zero to satisfy effectively the condition of mean ergodic theorem. For
391 eddies of 30 min and 60 min, which are larger scale, the mean ergodic function
392 $Ero(A)/A^*$ will deviate further from zero. In particular, the mean ergodic function
393 $Ero(A)/A^*$ of eddies of 30 min and 60 min for the temperature and humidity does not
394 converge, and even diverges. Above results show that the mean ergodic function of
395 eddies of 30 min and 60 min cannot converge to zero or cannot satisfy the condition
396 of mean ergodic theorem.

397 4.2.2 Comparison of the convergence of mean ergodic functions of vertical velocity,
398 temperature and humidity

399 As seen from the Figs. 1-3, dimensionless mean ergodic function of the vertical
400 velocity is compared with respective function of the temperature and humidity, it is
401 3-4 magnitudes less than those in the nocturnal stable boundary layer; 1-2 magnitudes
402 less than those in the early neutral boundary layer; and about 2 magnitudes less than
403 those in the midday convective boundary layer. For example, at 3:00-4:00 PM (CST)
404 during nighttime time frame, the dimensionless mean ergodic function of vertical
405 velocity is 10^{-5} in magnitude, while respective magnitudes of function value of the
406 temperature and humidity are 10^{-1} and 10^{-2} ; at 7:00-8:00 AM (CAT) during morning
407 time frame, magnitude of mean ergodic function of the vertical velocity is 10^{-4} , while
408 the respective magnitudes of function value of the temperature and humidity are 10^{-2}
409 and 10^{-3} ; at 13:00-14:00 PM(CST) during midday time frame, magnitude of mean
410 ergodic function of the vertical velocity is 10^{-4} , while the magnitudes of function
411 value of the temperature and humidity are both 10^{-2} . These results show that the
412 dimensionless mean ergodic function of vertical velocity converges to zero much

413 more easily than respective function value of the temperature and humidity, and that
414 the vertical velocity satisfies the condition of mean ergodic theorem to overmatch
415 more than the temperature and humidity.

416 4.2.3 Temporal scale and spatial scale of turbulent eddies

417 For wind velocity of 1-2 ms^{-1} , eddy spatial scale in the temporal scale 2 min is in the
418 range of 120-240 m, and eddy spatial scale in the temporal scale of 10 min is in the
419 range of 600-1200 m. The eddy spatial scale in the temporal scale of 2 min is
420 equivalent to ASL height, and the eddy spatial scale in the temporal scale of 10 min is
421 equivalent to ABL height. The eddy spatial scale within the temporal scales of 30-60
422 min is around 1800-3600 m, and this spatial scale clearly exceeds ABL height to
423 belong to scope of the atmospheric local circulation. According to the stationary
424 random processes definition (1) and mean ergodic theorem, the stationary random
425 processes must be smooth in relaxation time τ . The eddies below temporal scale of 10
426 min, i.e., below ABL height, are the stationary random processes, and can effectively
427 satisfy the condition of mean ergodic theorem. However, eddies in the temporal scales
428 of 30 min and 60 min exceed ABL height and do not satisfy the condition of mean
429 ergodic theorem, thus these eddies belong to the non-stationary random processes.

430 4.2.4 Turbulence ergodicity of all eddies in possible scales in ABL

431 To facilitate comparison, Fig. 4 shows the variation of mean ergodic function $\text{Ero}(A)$
432 of the vertical velocity (a), temperature (b) and specific humidity (c) before filtering
433 with relaxation time τ at 14:00-15:00 PM (CST) during midday time frame in
434 convective boundary layer. It is obvious that Fig. 4 is unfiltered mean ergodic
435 function of eddies in all possible scales in ABL. The Fig. 4 compares with Figs. 1c, 2c
436 and 3c, which are the mean ergodic function $\text{Ero}(A)/A^*$ of vertical velocity,
437 temperature and humidity after filtering at 14:00-15:00 PM (CST) during the midday
438 time frame. The result shows that the mean ergodic functions before filtering are
439 greater than that after filtering. As shown in Figs. 1c, 2c and 3c, the magnitude for the
440 vertical velocity is 10^{-4} and the magnitudes for the temperature and specific humidity
441 are both 10^{-2} . According to Fig. 4, the magnitude of vertical velocity $\text{Ero}(A)/A^*$ is 10^{-3}
442 and the magnitudes of temperature and specific humidity are both 10^0 , therefore 1-2
443 magnitudes are almost decreased after filtering. Moreover, all trend upward deviating
444 from zero for vertical velocity and temperature, but downward deviating from zero for
445 specific humidity. It is thus clear that, at 14:00-15:00 PM (CST) during the midday

446 time frame, when is equivalent to the local time 12:00-13:00, the unfiltered mean
447 ergodic function of eddies in all possible scales in convective boundary layer cannot
448 converge to zero before filtering, i.e., cannot satisfy the condition of mean ergodic
449 theorem. This may be that eddies in all possible scales before filtering include the
450 local circulation in convective boundary layer. So we argue that, under general
451 situations, the eddies only below 10 min in the temporal scale or within 600-1200 m
452 in the spatial scale in ABL are the ergodic stationary random processes, but also the
453 turbulence including the eddies with all possible scales in ABL may belong to the
454 non-ergodic stationary random processes.

455 4.2.5 Relation between the ergodicity and local stability of different scale eddies
456 Table 1 list the corresponding relation of eddy local stabilities z/L_c of eddies of
457 different scales with the different time frames. It shows that the eddy local stabilities
458 z/L_c of different scale eddies are different, due to the fact that the temperature
459 stratification in ABL has different effect on the stability for different scale eddies.
460 Even entirely contrary results can occur. At the same time, the stratification that
461 causes the large scale eddy to ascend with buoyancy may cause the small scale eddy
462 to descend. However, the results in Figs. 1-3 show that the ergodicity is mainly related
463 to the eddy scale, and its relation with the atmospheric temperature stratification
464 seems unimportance.

465 **4.3 Verification of autocorrelation ergodic theorem for different scale eddies**

466 In this section, Eqs. (7a) and (7b) are used to verify the autocorrelation ergodic
467 theorem. It is accordant with Sect. 4.2 that the turbulent eddies below 10 min in
468 temporal scale satisfy the mean ergodic condition in the various time frames, i.e., the
469 turbulent eddies below 10 min in temporal scale are at least strictly stationary random
470 processes or narrow stationary random processes whether in the nocturnal stable
471 boundary layer, or in the early neutral boundary layer and midday convective
472 boundary layer. Then we analyze further the different scale eddies that satisfy the
473 mean ergodic condition whether or not also satisfy the autocorrelation ergodic
474 condition, so as to verify atmospheric turbulence is whether narrow or wide stationary
475 random processes. The autocorrelation ergodic function of turbulence variable A
476 under the condition of truncated relaxation time $\tau_{i=n}$ is calculated according to Eq. (7a)
477 to determine the variation of autocorrelation ergodic function $Er(A)$ with relaxation
478 time τ . As with the mean ergodic function $Ero(A)$, if the autocorrelation ergodic

479 function $Er(A)$ of eddies of 2 min, 3 min, 5 min, 10 min, 30 min and 60 min in the
480 temporal scale within the relaxation time $\tau_{i=n}$ approximates 0, then A shall be deemed
481 to be approximately ergodic; the more the autocorrelation ergodic function deviates
482 from 0, the worse the autocorrelation ergodicity becomes. Therefore, this method can
483 be used to judge approximatively whether the different scale eddies satisfy the
484 condition of autocorrelation ergodic theorem.

485 As an example for the vertical velocity, Fig. 5 shows the variation of normalized
486 autocorrelation ergodic function $Ero(w)/u_*$ of the turbulent eddies of 2 min, 3 min, 5
487 min, 10 min, 30 min and 60 min in the temporal scale with relaxation time τ at
488 3:00-4:00, 7:00-8:00 and 13:00-14:00 (CST) during the time frames respectively.
489 Some basic conclusions are drawn from Fig. 5 as following:

- 490 1. After comparing the Figs. 5a-c with the Figs. 1a-c, i.e., comparing the
491 dimensionless mean ergodic function $Ero(w)/u_*$ of vertical velocity with the
492 dimensionless autocorrelation ergodic function $Er(w)/u_*$, two basic characteristics
493 are very clear. First, the magnitudes of the dimensionless autocorrelation ergodic
494 function $Er(w)/u_*$, regardless of whether in the nocturnal stable boundary layer,
495 early neutral boundary layer or midday convective boundary layer, are all greatly
496 reduced. In Figs. 1a-c, the magnitudes of $Ero(w)/u_*$ are respectively 10^{-5} , 10^{-4} and
497 10^{-4} , and the magnitudes of $Er(w)/u_*$ are respectively 10^{-7} , 10^{-5} and 10^{-5} as shown in
498 Figs. 5a-c. The magnitudes of $Er(w)/u_*$ reduce by 1-2 magnitudes compared with
499 those of $Ero(w)/u_*$. Second, all autocorrelation ergodic functions $Er(w)/u_*$ of the
500 eddies of 30 min and 60 min in temporal scale, regardless of whether they are in
501 the stable boundary layer, natural boundary layer or convective boundary layer, are
502 all reduced and approximate to $Ero(w)/u_*$ of the eddies below 10 min in temporal
503 scale.
- 504 2. The above two basic characteristics imply that the autocorrelation ergodic function
505 $Er(w)/u_*$ of the stable boundary layer, neutral boundary layer or convective
506 boundary layer converges to 0 faster than the mean ergodic function $Ero(w)/u_*$; the
507 autocorrelation ergodic function of eddies of 30 min and 60 min in temporal scale
508 also converges to 0 and satisfies the condition of autocorrelation ergodic theorem,
509 except for the fact that the autocorrelation ergodic function $Er(w)/u_*$ of the eddies
510 below 10 min in temporal scale can converge to 0 and satisfy the condition of
511 autocorrelation ergodic theorem.

512 3. According to the autocorrelation ergodic function Eq. (7a), the eddies of 30 min, 60
513 min and below 10 min in the temporal scale, regardless of whether they are in the
514 stable boundary layer, neutral boundary layer or convective boundary layer, all
515 eddies satisfy the condition of autocorrelation ergodic theorem. Therefore, in
516 general ABL turbulence is the stationary random processes of autocorrelation
517 ergodicity.

518 4. The above results show that the eddies below 10 min in temporal scale in the
519 nocturnal stable boundary layer, early neutral boundary layer and midday
520 convective boundary layer do not only satisfy the condition of mean ergodic
521 theorem, but also they satisfy the condition of autocorrelation ergodic theorem.
522 Therefore, eddies below 10 min in the temporal scale are a wide ergodic stationary
523 random processes. Although the eddies of 30 min and 60 min in temporal scale in
524 the stable boundary layer, neutral boundary layer and convective boundary layer
525 satisfy the condition of autocorrelation ergodic theorem, but they dissatisfy the
526 condition of mean ergodic theorem. Therefore, eddies of 30 min and 60 min in the
527 temporal scale are neither narrow ergodic stationary random processes, nor wide
528 ergodic stationary random processes.

529 **4.4 Ergodic theorem verification of different scale eddies for the multi-stations**

530 The basic principle of turbulence average is an ensemble average of the space, time
531 and state. Sections 4.2 and 4.3 verify the mean ergodic theorem and autocorrelation
532 ergodic theorem of atmospheric turbulence using field observational data, so that the
533 finite time average of a single station can be used to substitute for the ensemble
534 average for the ergodic turbulence. This section examines the ergodicity of different
535 scale eddies using the observational data of center tower and six sub-sites of
536 CASES-99, in all seven sites to be equivalent to seven stations. When the data are
537 selected, it is considered that if the eddies are not evenly distributed at the seven sites,
538 then the observation results at the seven sites may have originated from many eddies
539 in the large scale. For this reason, the high frequency variance spectrum above 0.1 Hz
540 is compared firstly. Based on the observational error, if the scatter of all high
541 frequency variances does not exceed the average by $\pm 10\%$, then it is assumed that the
542 turbulence is evenly distributed at the seven observation sites. And then, 17 datasets
543 are chosen from among the observed turbulence data from 5 to 30 October, and these
544 data sets represent typical strong turbulence at noon on the sunny day. As an example,

545 the same method as described in Sections 4.2 and 4.3 is used to respectively calculate
546 variation of the mean ergodic function and autocorrelation ergodic function with
547 relaxation time τ for the vertical velocity at 10:00-11:00 AM on 7 October. The time
548 series composed of the above data sets is performed band-pass filtering in 2 min, 3
549 min, 5 min, 10 min, 30 min and 60 min. The variations of mean ergodic function
550 $Ero(w)/u_*$ and autocorrelation ergodic function $Er(w)/u_*$ with relaxation time τ are
551 analyzed for the vertical velocity to test the ergodicity of different scale eddies for
552 observation of the multi-stations. Fig. 6a shows variation of mean ergodic function
553 $Ero(w)/u_*$ with the relaxation time τ for the vertical velocity, and Fig. 6b shows
554 variation of autocorrelation ergodic function $Er(w)/u_*$ with the relaxation time τ .

555 The results show ergodic characteristics of different scale eddies measured with the
556 multi-stations as following:

557 Fig. 6a shows that the mean ergodic function of eddies below 30 min in temporal
558 scale converges to 0 very well, except for the fact that the mean ergodic function of
559 eddies of 60 min in temporal scale clearly deviates upward from 0. Fig. 6b shows that
560 autocorrelation ergodic function of all different scale eddies including 60 min in
561 temporal scale, gradually converges to 0. Therefore, eddies below 30 min in temporal
562 scale measured with the multi-stations satisfy the conditions of both the mean and
563 autocorrelation ergodic theorem, while eddies of 60 min in temporal scale only
564 satisfies the condition of autocorrelation ergodic theorem, but dissatisfy the condition
565 of mean ergodic theorem. These facts demonstrate that eddies below 30 min in
566 temporal scale are the wide ergodic stationary random processes for time series of
567 above data sets composed by the seven stations. This signifies that comparing of data
568 composed of the multi-stations with data from a single station, the eddy temporal
569 scale of wide ergodic stationary random processes is extended from below 10 min to
570 30 min. As analyzed above, if the eddies below 10 min in temporal scale are deemed
571 to be the turbulent eddies in the ABL with height about 1000 m, and the eddies of 30
572 min in the temporal scale, which is equivalent to that the space scale is greater than
573 2000 m, are deemed including eddy components of the local circulation in ABL, in
574 that way the multiple station observations can completely capture the local circulated
575 eddies, which space scale is greater than 2000 m.

576 **4.5 Average time problem of turbulent quantity averaging**

577 The atmospheric observations are impossible to repeat experiments exactly, must use

578 the ergodic hypothesis and replace ensemble averages with time averages. It arises a
579 problem how does determine the averaging time.

580 The analyses on the ergodicity of different scale eddies in above two sections
581 demonstrate that the eddies below 10 min in temporal scale as relaxation time $\tau=30$
582 min in the stable boundary layer, neutral boundary layer and convective boundary
583 layer not only satisfy the mean ergodic theorem, but also satisfy the autocorrelation
584 ergodic theorem. That is to say, they are namely wide ergodic stationary random
585 processes. Therefore, a finite time average of 30 min within relaxation time τ can be
586 used for substituting for the ensemble average to calculate mean random variable, Eq.
587 (2). However, the eddies of 30 min and 60 min in temporal scale in the stable
588 boundary layer and neutral boundary layer are only autocorrelation ergodic random
589 processes, neither narrow nor wide sense random processes. Therefore, when the
590 finite time average of 30 min can be used for substituting for the ensemble average to
591 calculate mean random variable Eq. (2), it may capture the eddies below 10 min in
592 temporal scale in stationary random processes, but cannot completely capture the
593 eddies above 30 min in temporal scale. The above results signify that the turbulence
594 average is restricted not only by the mean ergodic theorem, but also is closely related
595 to the scale of turbulent eddies. In the atmospheric observations performed using the
596 eddy-covariance technique, the substitution of ensemble average with finite time
597 average of 30 min inevitably results in a high level of error, due to loss of low
598 frequency component information associating with the large-scale eddies. However,
599 although eddies of 30 min and 60 min in temporal scale in convective boundary layer
600 are not wide ergodic stationary random processes, they are autocorrelation ergodic
601 random processes. This may imply that the mean of atmospheric turbulence in the
602 convective boundary layer, which is calculated to substitute the finite time average for
603 the ensemble average, is often superior to the results of the stable boundary layer and
604 neutral boundary layer. Withal, the results in the previous sections also show that the
605 mean ergodic function of vertical velocity may more easily converge to 0 than
606 functions corresponding to the temperature and humidity, i.e., the vertical velocity
607 may more easily satisfy the condition of mean ergodic theorem than the temperature
608 and humidity. Therefore, in the observation performed using the eddy-covariance
609 technique, the result of vertical velocity is often superior to those of the temperature
610 and humidity. In the previous section, the results also point out that multi-stations

611 observation can completely capture eddy of the local circumfluence in the ABL.
 612 Therefore, the multi-stations observation is more likely to satisfy the ergodic
 613 assumption, and its results are much closer to the true values. In order to determine
 614 the averaging time, Oncley (1996) defined an Ogive function of cumulative integral

$$615 \quad Og_{x,y}(f_0) = \int_{\infty}^{f_0} Co_{x,y}(f) df \quad (15)$$

616 where x and y are any two variables, and their covariance is \bar{xy} , $Co_{xy}(f)$ is the
 617 cospectrum of xy . If the Ogive function converges to a constant value at a frequency
 618 $f=f_0$, this frequency could be converted to an averaging time. Ogive function of $\bar{u'w'}$
 619 is often used to examine the minimal averaging time. As a comparison, here the
 620 variation of Ogive functions of $\bar{w'^2}$ and $\bar{u'w'}$ with frequency at the height 3.08 m in
 621 NSPCE/CAS for the three time frames is shown in Fig.7. The Fig.7 shows
 622 convergence frequency of Ogive function for $\bar{w'^2}$ in the nighttime stable boundary
 623 layer, morningtide neutral boundary layer and midday convection boundary layer is
 624 respectively about at 0.01 Hz, 0.0001 Hz and 0.001 Hz. It is equivalent to the
 625 averaging times about 2 min, 160 min and 16 min. For $\bar{u'w'}$, it converges about at
 626 0.001 Hz only in the midday convection boundary layer to be equivalent to the
 627 averaging time about 16 min; it seems no convergence in the nighttime stable and
 628 morningtide neutral boundary layer. It is implied determining the averaging time
 629 encounters a bit difficult with the Ogive function in the stable and neutral boundary
 630 layer. Fig.7 shows also that when the frequency is lower than 0.0001Hz, Ogive
 631 functions $\bar{u'w'}$ ascend in the stable boundary layer, but descend in the morningtide
 632 neutral boundary layer and midday convection boundary layer. We must especially
 633 note that Ogive function is a cumulative integral. So as Ogive function changes
 634 direction from ascending to descending, it implies a possibility that there exists a
 635 superimposing of the negative and positive momentum fluxes caused by a cross local
 636 circulation effect in nighttime and midday. This cross local circulation in ABL may
 637 cause the low frequency effect on the Ogive function. So that the local circulation in
 638 ABL may be an important cause that Ogive fails to judge the averaging time. In this
 639 work, the choice of averaging time with the ergodic theory seems superior to with the
 640 Ogive function.

641 **4.6 MOS of turbulent eddies in different scales and its relation with ergodicity**

642 Turbulent variance is a most basic characteristic quantity of the turbulence.
 643 Turbulence velocity variance, which represents turbulence intensity, and the variance
 644 of scalars, such as temperature and humidity, effectively describes the structural
 645 characteristics of turbulence. In order to test MOS relation of the different scale
 646 eddies with ergodicity, the vertical velocity and temperature data of NSPCE/CAS
 647 from 23 July to 13 September are used to determine the MOS relationship of
 648 variances of vertical velocity and temperature for the different scale eddies, and to
 649 analyze its relation with the ergodicity.

650 The MOS relation of vertical velocity variance as following:

651 $\phi_i(z/L) = c_1(1 - c_2 z/L)^{1/3}, \quad z/L < 0, \quad (16)$

652 $\phi_i(z/L) = c_1(1 + c_2 z/L)^{1/3}, \quad z/L > 0. \quad (17)$

653 Fig. 8 and 9 respectively shows the MOS relation curves of different scale eddies for
 654 the vertical velocity and temperature variances in NSPCE/CAS. The figures (a), (b)
 655 and (c) of Fig. 8 and 9 are respectively the similarity curve of eddies of 10 min, 30
 656 min and 60 min in the temporal scale. Table 2 shows the relevant parameters of fitting
 657 curve of MOS relation for the vertical velocity variance. The correlation coefficient
 658 and residual of fitting curve are respectively expressed with R and S .

659 Fig. 8 and Table 2 show that the parameters of fitting curve are greatly different,
 660 even if the fitting curve modality of MOS relation of the vertical velocity variance is
 661 the same for the eddies in different temporal scales. The correlation coefficients of
 662 MOS fitting curve of the vertical velocity variance under the unstable stratification are
 663 large, but the correlation coefficients under the stable stratification are small. Under
 664 unstable stratification, the correlation coefficient of eddies of 10 min in the temporal
 665 scale reaches 0.97, while the residual is only 0.16; under the stable stratification, the
 666 correlation coefficient reduces to 0.76, and the residual increases to 0.25. With the
 667 increase of eddy temporal scale from 10 min (Fig. 8a) to 30 min (Fig. 8b) and 60 min
 668 (Fig. 8c), the correlation coefficients of MOS relation of the vertical velocity variance
 669 gradually reduce, and the residuals increase. The correlation coefficient in 60 min
 670 reaches a minimum; it is 0.83 under the unstable stratification, and only 0.30 under
 671 the stable stratification.

672 The temperature variance is shown in Fig. 9. MOS function to fit from eddies of 10
 673 min in the temporal scale under the unstable stratification is following:

674 $\phi_\theta(z/L_c) = 4.9(1 - 79.7z/L_c)^{-1/3}$. (18)

675 As shown in Fig. 9a, the correlation coefficient of fitting curve is 0.91 and residual is
 676 0.38. With increase of the eddy temporal scale, discreteness of MOS relation of the
 677 temperature variance is enlarged quickly to incur that the appropriate curve cannot be
 678 fitted.

679 The above results show that the discreteness of fitting curve of MOS relation for
 680 the turbulence variance is enlarged with the increase of eddy temporal scale, whether
 681 it is the vertical velocity or temperature. The points of data during the stationary
 682 processes basically gather nearby the fitting curve of variance similarity relation,
 683 while all data points during the non-stationary processes deviate significantly from the
 684 fitting curve. However, the similarity of vertical velocity variance is superior to that of
 685 the temperature variance. These results are consistent to the conclusions of ergodicity
 686 test for the different scale eddies described in Sections 4.2-4.4. The ergodicity of the
 687 small-scale eddies is superior to that of the larger-scale eddies, and eddies of 10 min
 688 in the temporal scale have the best variance similarity relations. These results also
 689 signify that when eddies in the stationary random processes satisfy the ergodic
 690 condition, both the vertical velocity variance and temperature variance of eddies in the
 691 different temporal scales comply with MOST very well; but, as for eddies with poor
 692 ergodicity during non-stationary random processes, the variances deviate from MOS
 693 relations.

694 **5 Conclusions**

695 From the above results, we can draw the below preliminary conclusions:

- 696 1. The turbulence in ABL is an eddy structure. When the temporal scale of turbulent
 697 eddies in ABL is about 2 min, the corresponding spatial scale is about 120-240 m
 698 to be equivalent to ASL height; when the temporal scale of turbulent eddies in ABL
 699 is about 10 min, the corresponding spatial scale is about 600-1200 m to be
 700 equivalent to the ABL height. For the eddies of larger temporal and spatial scale,
 701 such as eddies of 30-60 min in the temporal scale, the corresponding spatial scale
 702 is about 1800-3600 m to exceed the ABL height.
- 703 2. The above results show that the ergodicity of atmospheric turbulence in ABL is not
 704 only relative to the atmospheric stratification but also to the eddy scale of
 705 atmospheric turbulence. For the atmospheric turbulent eddies below the ABL scale,
 706 i.e. the eddies below about 1000 m in the spatial scale and about 10 min in the

707 temporal scale, the mean ergodic function $Ero(A)$ and autocorrelation ergodic
708 function $Er(A)$ converge to 0, i.e., they satisfy the conditions of mean and
709 autocorrelation ergodic theorem. However, for the atmospheric turbulent eddies
710 above 2000-3000 m in the spatial scale and above 30-60 min in the temporal scale,
711 the mean ergodic function doesn't converge to 0, thus dissatisfy the condition of
712 mean ergodic theorem. Therefore, the turbulent eddies that is below the ABL scale
713 belong to the wide ergodic stationary random processes, but the turbulent eddies
714 that are larger than ABL scale belong to the non-ergodic random processes, or even
715 the non-stationary random processes.

716 3. Due to above facts, when the stationary random process information of eddies
717 below 10 min in the temporal scale and below 1000 m of ABL height in the spatial
718 scale can be captured, the atmospheric turbulence may satisfy the condition of
719 mean ergodic theorem. Therefore, an average of finite time can be used to
720 substitute for the ensemble average to calculate the mean of random variable as
721 measuring atmospheric turbulence with the eddy-covariance technique. But for the
722 turbulence of eddies to be larger than 30 min in temporal scale, i.e., 2000 m in
723 spatial scale magnitude, it dissatisfy the condition of mean ergodic theorem, so that
724 the eddy-covariance technique cannot completely capture the information of
725 non-stationary random processes. This will inevitably cause a high level of error
726 when the average of finite time is used to substitute for the ensemble average in the
727 experiments due to the loss of low frequency component information associating
728 with the large-scale eddies.

729 4. Although the atmospheric temperature stratification has different effects on the
730 stability of eddies in the different scales, the ergodicity is mainly related to the
731 eddy local stability, and its relation with the stratification stability of ABL is not
732 significant.

733 5. The data series composed from seven stations compare with the observational data
734 from a single station. The results show that the temporal and spatial scale of eddies
735 to belong to the wide ergodic stationary random processes are extended from 10
736 min to below 30 min and from 1000 m to below 2000 m respectively. This signifies
737 that the ergodic assumption is more likely to be satisfied well with multi-stations
738 observation, and observational results produced by the eddy-covariance technique
739 are much closer to the true values when calculating the turbulence averages,

740 variances or fluxes.

741 6. If the ergodic conditions of stationary random processes are more effectively
742 satisfied, then the turbulence variances of eddies in the different temporal scale
743 can comply with MOST very well; however, the turbulence variances of the
744 non-ergodic random processes deviate from MOS relations.

745

746 6 Discussions

747 1. Galanti and Tsinober (2004) proved that the turbulence, which is temporally steady
748 and spatially homogeneous, is ergodic, but '*partially turbulent flows*' such as the
749 mixed layer, wake flow, jet flow, flow around and boundary layer flow may be
750 non-ergodic turbulence. However, it has been proven through atmospheric
751 observational data that the turbulence ergodicity is related to the scale of turbulent
752 eddies. Since the large-scale eddies in ABL may be strongly influenced by the
753 boundary disturbance, thus belong to '*partial turbulence*'; however, since the
754 small-scale eddies in atmospheric turbulence may be not influenced by boundary
755 disturbance, may be temporally steady and spatially homogeneous turbulence. So
756 that the mean ergodic theorem and autocorrelation ergodic theorem are applicative
757 for turbulence eddies in the small scale in ABL, but the ergodic theorems aren't
758 applicative for the large-scale eddies, i.e., the small-scale eddies in the ABL are
759 ergodic and the large-scale eddies exceeding the ABL scale are non-ergodic.

760 2. The eddy-covariance technique for turbulence measurement is based on the ergodic
761 assumption. A lack of ergodicity related to the presence of large-scale eddy
762 transport can lead to a consider error of the flux measurement. This has already
763 been pointed out by Mauder et al. (2007) or Foken et al. (2011). Therefore, we
764 realize from the above conclusions that the large scale eddies that exceed ABL
765 height may include component of non-ergodic random processes. The
766 eddy-covariance technique cannot capture the signals of large-scale eddies
767 exceeded ABL scale, thus resulting in the large error in the measurements of
768 atmospheric turbulent variance and covariance. MOST is developed under the
769 condition of the steady time and homogeneous surface. MOST conditions, steady
770 time and homogeneous underlying surface, are in line with the ergodic conditions,
771 therefore the turbulence variances, even the turbulent fluxes of eddies in different
772 temporal scales may comply with MOST very well, if the ergodic conditions of
773 stationary random processes are more effectively satisfied.

774 3. According to Kaimal and Wyngaard (1990), the atmospheric turbulence theory and
775 observation method were feasible and led to success under ideal conditions
776 including a short period, steady state and homogeneous underlying surface, and
777 through observation in the 1950s-1970s, but these conditions are rare in reality. In
778 the land surface processes and ecosystem, the turbulent flux observations in ASL
779 turn into a scientific issue, in which commonly interest researchers in the fields of
780 atmospheric sciences, ecology, geography sciences, etc. These observations must
781 be implemented under conditions such as with complex terrain, heterogeneous
782 surface, long period and unsteady state. It is necessary that more neoteric
783 observational tools and theories will be applied with new perspectives in future
784 research.

785 4. It is successful that the ergodic theorem of stationary random processes is
786 introduced from the mathematics into atmospheric sciences. It undoubtedly
787 provides a profited tool for overcoming the challenges encountering in the modern
788 measurements of atmospheric turbulent flow. At least it offers a promising first step
789 to diagnosticate directly the ergodic hypotheses for ASL flows as a criterion. And
790 that the necessary and sufficient condition of ergodic theorem can be used to judge
791 the applicative scope of eddy-covariance technique and MOST, and seek potential
792 disable reasons for using them in the ABL.

793 5. In the future, we shall keep up to study the ergodic problems for the atmospheric
794 turbulence measurements under the conditions of complex terrain, heterogeneous
795 surface and unsteady, long observational period, and to seek effective schemes. The
796 above results indicate the atmospheric turbulent eddies below the scale of ABL can
797 be captured by the eddy-covariance technique and comply with MOST very well.
798 Perhaps MOST can be as the first order approximation to deal with the turbulence
799 of eddies below ABL scale satisfying the ergodic theorems, then to compensate the
800 effects of eddies dissatisfying the ergodic theorem, which may be caused by the
801 advection, local circulation, low frequency effect, etc. under the complex terrain,
802 heterogeneous surface. For example, we developed a turbulent theory of
803 non-equilibrium thermodynamics (Hu, Y., 2007; Hu, Y., et al., 2009) to find the
804 coupling effects of vertical velocity, which is caused by the advection, local
805 circulation, and low frequency, on the vertical fluxes. The coupling effects of
806 vertical velocity may be as a scheme to compensate the effects of eddies

807 dissatisfying the ergodic theorems (Hu, Y., 2003; Chen, J., et al., 2007, 2013).
808 6. It is clear that such studies are preliminary, and many problems require further
809 research, and the attestation of more field experiments is necessary.

810
811 *Acknowledgements.* This study is supported by Project Granted Nos. 91025011,
812 91437103 of the National Natural Science Foundation of China and Project Granted
813 No. 2010CB951701-2 of the National Program on Key Basic Research. This work
814 was strongly supported by Heihe Upstream Watershed Ecology-Hydrology
815 Experimental Research Station, Chinese Academy of Sciences. We would like to
816 express my sincere regards for their support. And that we thank Dr. Gordon Maclean
817 in NCAR for providing the detailed data of CASES-99 used in this study, and thank
818 referees and editor very much for heartfelt comments, discussions and marked errors.

819
820 References

821 Aubinet, M., Vesala, T., and Papale, D.: Eddy covariance, a practical guide to
822 measurement and data analysis, Springer, Dordrecht, Heidelberg, London, New
823 York, 438 pp., 2012.
824 Birkhoff, G. D.: Proof of the ergodic theorem, P. Natl. Acad. Sci. USA, 18, 656-660,
825 1931.
826 Boltzmann, L.: Analytischer beweis des zweiten Haubtsatzes der mechanischen
827 Wärmetheorie aus den Sätzen über das Gleichgewicht der lebendigen Kraft, Wiener
828 Berichte , 63, 712-732, in WAI, paper 20, 1871.
829 Chang, S. S. and Huynh, G. D.: Analysis of sonic anemometer data from the
830 CASES-99 field experiment. Army Research Laboratory, Adelphi, MD. 2002.
831 Chen, J., Hu, Y., and Zhang, L.: Principle of cross coupling between vertical heat
832 turbulent transport and vertical velocity and determination of cross coupling
833 coefficient, Adv. Atoms. Sci., 23, 639-648, 2007.
834 Chen, J., Hu, Y., Lu, S., and Yu, Ye.: Experimental demonstration of the coupling
835 effect of vertical velocity on latent heat flux, Sci. China. Ser. D-Earth Sci., 56,

836 1-9, 2013.

837 Eichinger, W. E., Parlange, M. B., Katul, G. G.: Lidar measurements of the
838 dimensionless humidity gradient in the unstable ASL, Lakshmi, V., Albertson, J.
839 and Schaake, J., Koster, R. D., Duan, Q., Land Surface Hydrology, Meteorology,
840 and Climate, American Geophysical Union, Washington, D. C. 7-13, 2001.

841 Ehrenfest, P., Ehrenfest-Afanassjewa, T.: The conceptual foundations of the statistical
842 approach in mechanics, Cornell University Press, New York, 114 pp., 1959.

843 Foken, T., Wichura, B.: Tools for quality assessment of surface-based flux
844 measurements. Agric. For. Meteorol., 78, 83-105, 1996.

845 Foken, T., Göckede, M., Mauder, M., Mahrt, L., Amiro, B. D., and Munger, J. W.:
846 Post-field data quality control, in: Handbook of micrometeorology: a guide for
847 surface flux measurement and analysis, Lee, X., Massman, W. J., and Law, B.:
848 Kluwer, Dordrecht, 181-208, 2004.

849 Foken, T., Aubinet, M., Finnigan, J. J., Leclerc, M. Y., Mauder, M., Paw, U. K. T.:
850 Results of a panel discussion about the energy balance closure correction for
851 trace gases. Bull. Am. Meteorol. Soc., 92, ES13-ES18, 2011.

852 Galanti, B. and Tsinober, A.: Is turbulence ergodic? Phys. Lett. A, 330, 173–18, 2004.

853 Higgins, C. W., Katul, G. G., Froidevaux, M., Simeonov, V. and Parlange, M. B.: Are
854 atmospheric surface layer flows ergodic? Geophy. Res. Lett., 40, 3342-3346,
855 2013.

856 Hill, R. J.: Implications of Monin–Obukhov similarity theory for scalar quantities, J.
857 Atmos. Sci. 46, 2236–2244, 1989.

858 Hu, Y.: Convergence movement influence on the turbulent transportation in
859 atmospheric boundary layer, Adv. Atoms. Sci., 20, 794-798, 2003.

860 Hu, Y., Chen, J., Zuo, H.: Theorem of turbulent intensity and macroscopic mechanism

861 of the turbulence development, *Sci. China Ser. D-Earth Sci.*, **37**, 789-800, 2007.

862 Hu, Y., and Chen, J.: *Nonequilibrium Thermodynamic Theory of Atmospheric*
863 *Turbulence*, In: *Atmospheric Turbulence, Meteorological Modeling and*
864 *Aerodynamics*, Lang P., R. and Lombargo, F., S., Nova Science Publishers, New
865 York,, 59-110, 2010.

866 Kaimal, J. C. and Wyngaard, J. C.: The Kansas and Minnesota experiments,
867 *Bound.-Lay. Meteorol.*, 50, 31-47, 1990.

868 Kaimal, J. C. and Gaynor, J. E.: Another look at sonic thermometry, *Bound.-Lay.*
869 *Meteorol.*, 56, 401–410, 1991.

870 Katul, G. G., Hsieh, C. I.: A note on the flux-variance similarity relationships for heat
871 and water vapor in the unstable atmospheric surface layer, *Bound.-Lay. Meteorol.*,
872 90, 327–338, 1999.

873 Katul, G., Cava, D., Poggi, D., Albertson, J., and Mahrt, L.: Stationarity, homogeneity,
874 and ergodicity in canopy turbulence, in: *Handbook of micrometeorology: a guide*
875 for surface flux measurement and analysis, Lee, X., Massman, W. J., and Law, B.:
876 Kluwer, Dordrecht, 161–180, 2004.

877 Krengel, U.: *Ergodic theorems*, de Gruyter, Berlin, New York, 363 pp., 1985.

878 Lennaert van, V., Shigeo, K., and Genta, K.: Periodic motion representing isotropic
879 turbulence, *Fluid Dyn. Res.*, 38, 19–46, 2006.

880 Li, X., Hu, F., Pu, Y., Al-Jiboori, M. H., Hu, Z., and Hong, Z.: Identification of
881 coherent structures of turbulence at the atmospheric surface layer, *Adv. Atoms.*
882 *Sci.*, 19, 687-698, 2002.

883 Martano, P.: Estimation of surface roughness length and displacement height from
884 single-level sonic anemometer data, *J. Appl. Meteorol.*, 39, 708–715, 2000.

885 Mattingly, J. C.: On recent progress for the stochastic Navier Stokes equations,

886 Journées équations aux dérivées partielles, Univ. Nantes., Nantes., Exp. No. XI,
887 1-52, 2003.

888 Mauder, M., Desjardins, R. L., MacPherson, I.: Scale analysis of airborne flux
889 measurements over heterogeneous terrain in a boreal ecosystem. *J. Geophys.*
890 *Res.-ATMOS.*, 112, D13, 2007.

891 McMillen, R. T.: An eddy correlation technique with extended applicability to non
892 simple terrain, *Bound.-Lay. Meteorol.*, 43, 231-245, 1988.

893 Moore, C. J.: Frequency response corrections for eddy correlation systems,
894 *Bound.-Lay. Meteorol.*, 37, 17-35, 1986.

895 Neumann, J. V.: Proof of the quasi-ergodic hypothesis, *P. Natl. Acad. Sci. USA*, 18,
896 70-82, 1932.

897 Oncley, S. P., Friehe, C. A., LaRue, J. C., Businger, J. A., Itsweire, E. C., Chang, S. S.:
898 Surface-layer fluxes, profiles, and turbulence measurements over uniform terrain
899 under near-neutral conditions, *J. Atmos. Sci.*, 53, 1029-1044, 1996.

900 Padro, J.: An investigation of flux-variance methods and universal functions applied
901 to three land-use types in unstable conditions, *Bound.-Lay. Meteorol.*, 66,
902 413–425, 1993.

903 Panofsky, H. A., Lenschow, D. H., and Wyngaard, J. C.: The characteristics of
904 turbulent velocity components in the surface layer under unstable conditions.
905 *Bound.-Lay. Meteorol.*, 11, 355–361, 1977.

906 Papoulis, A. and Pillai, S. U.: *Probability, random variables and stochastic processes*.
907 McGraw Hill. New York. 666 pp., 1991.

908 Poulos, G. S., Blumen, W., Fritts, D. C., Lundquist, J. K., Sun, J., Burns, S. P., Nappo,
909 C., Banta, R., Newsom, R., Cuxart, J., Terradellas, E., and Balsley, Ben.: CASES-99:
910 A comprehensive investigation of the stable nocturnal boundary layer. *Bull Am.*

911 Meteorol. Soc., 83, 555–581, 2002.

912 Schotanus, P., Nieuwstadt, F. T. M., and de Bruin, H. A. R.: Temperature measurement
913 with a sonic anemometer and its application to heat and moisture fluxes,
914 Bound.-Lay. Meteorol., 26, 81–93, 1983.

915 Stull, R. B.: An introduction to boundary layer meteorology. Kluwer Academic Publ.
916 Dordrecht. 670 pp., 1988.

917 Uffink, J.: Boltzmann'S work in statistical physics, Stanford encyclopedia of
918 philosophy, Edward, N. Z., 2004.
919 <http://plato.stanford.edu/entries/statphys-Boltzmann/>

920 Vickers, D., Mahrt, L.: Quality control and flux sampling problems for tower and
921 aircraft data. J. Atmos. Ocean. Tech., 14, 512-526, 1997.

922 Webb, E. K., Pearman, G. I., and Leuning, R.: Correction of the flux measurements for
923 density effects due to heat and water vapor transfer, Q. J. Roy. Meteor. Soc., 106,
924 85–100, 1980.

925 Wilczak, J. M., Oncley, S. P., Stage, S. A.: Sonic anemometer tilts correction
926 algorithms. Bound.-Lay. Meteorol., 99, 127-150, 2001.

927 Wyngaard, J. C.: Turbulence in the atmosphere, getting to know turbulence,
928 Cambridge University Press, New York, 393 pp. 2010.

929 Zuo, H., Xiao X., Yang Q., Dong L., Chen J., Wang S.: On the atmospheric movement
930 and the imbalance of observed and calculated energy in the surface layer, Sci. China
931 Ser. D-Earth Sci., 55, 1518-1532, 2012.

932

933

Table 1 Local Stability Parameter $(z-d)/L_c$ of the Eddies in Different Temporal Scales on 25 August

Time	3:00-4:00	7:00-8:00	14:00-15:00
Eddy scale			
≤ 2 min	0.59	0.52	-0.38
≤ 3 min	0.31	0.38	-0.44
≤ 5 min	0.28	0.16	-0.40
≤ 10 min	-0.01	0.15	-0.34
≤ 30 min	-0.04	-0.43	-0.27
≤ 60 min	-0.07	-1.29	-0.30

934

Table 2 Parameters of the Fitting Curve of MOS relation for Vertical Velocity Variance

	10 min		30 min		60 min	
	$z/L < 0$	$z/L > 0$	$z/L < 0$	$z/L > 0$	$z/L < 0$	$z/L > 0$
c_1	1.08	1.17	1.06	1.12	0.98	1.06
c_2	4.11	3.67	3.64	3.27	4.62	2.62
R	0.97	0.76	0.94	0.56	0.83	0.30
S	0.19	0.25	0.17	0.27	0.25	0.31

935

936

937

938

939

940

941

942

943

944

945

946

947

948

949

950

951

952

953

954

955

956

957

958

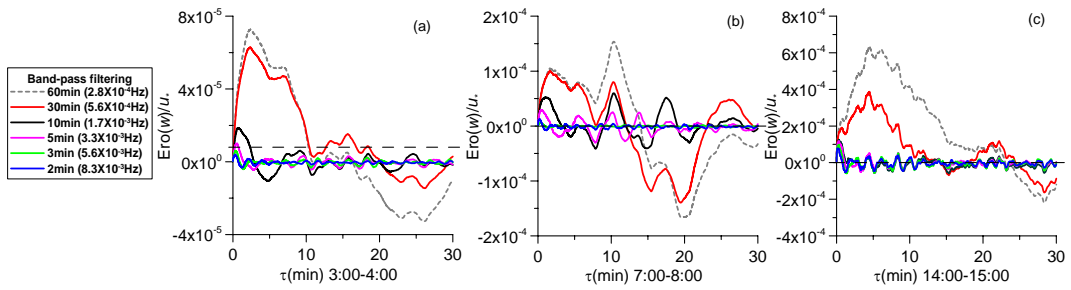


Fig. 1. Variation of mean ergodic function $Ero(w)$ of vertical velocity measured at the height 3.08 m in NSPCE with relaxation time for the different scale eddies after band-pass filtering. Panels (a), (b) and (c) are the respective results of the three time frames. If their mean ergodic function is more approximate to zero, then eddies in the corresponding temporal scale will more closely satisfy the ergodic conditions.

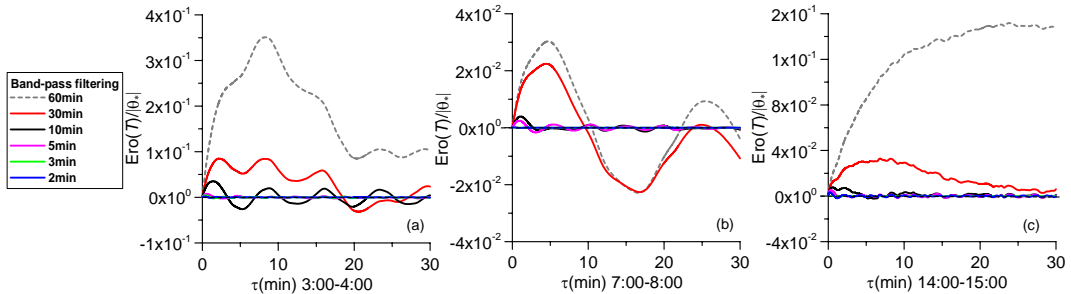


Fig. 2. Variation of mean ergodic function $Ero(T)$ of the different scale eddies of temperature with relaxation time (other conditions are as some as Fig. 2, and the same applies to the following figures).

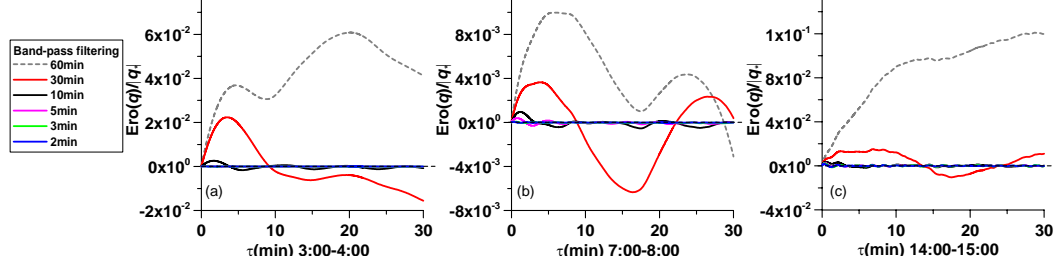


Fig. 3. Variation of mean ergodic function $Ero(q)$ of the different scale eddies of humidity with relaxation time.

969

970

971

972

973

974

975

976

977

978

979

980

981

982

983

984

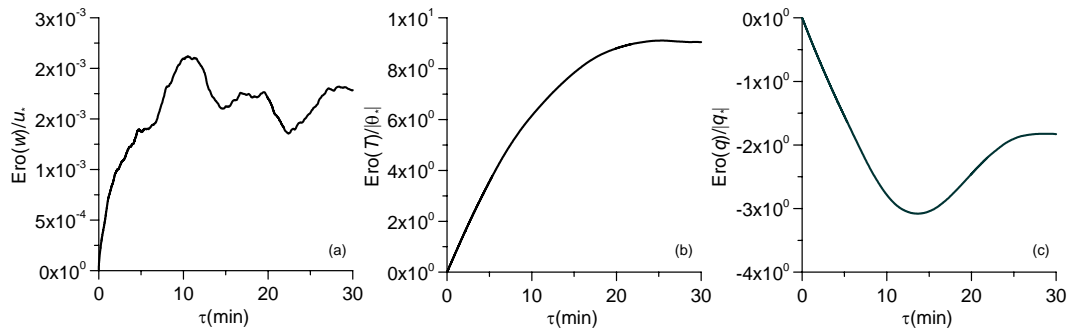


Fig. 4. Variation of mean ergodic function $Ero(w)$ of the vertical velocity (a), temperature (b) and specific humidity (c) before filtering at 14:00-15:00 (CST) during midday in NSPCE with relaxation time τ .

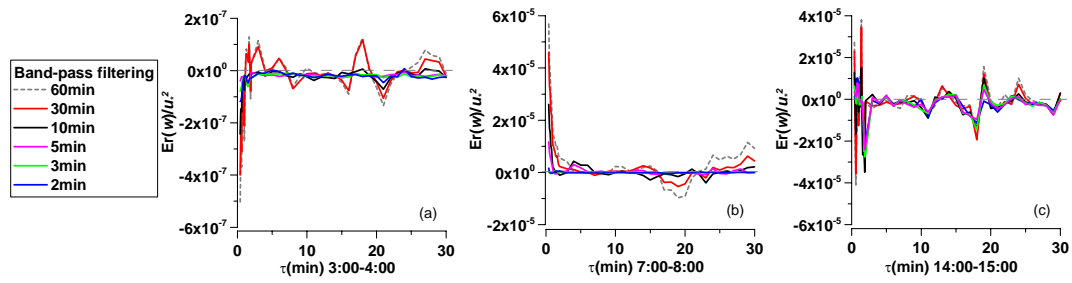


Fig. 5. Variation of the autocorrelation ergodic function of vertical velocity with relaxation time for different scale eddies.

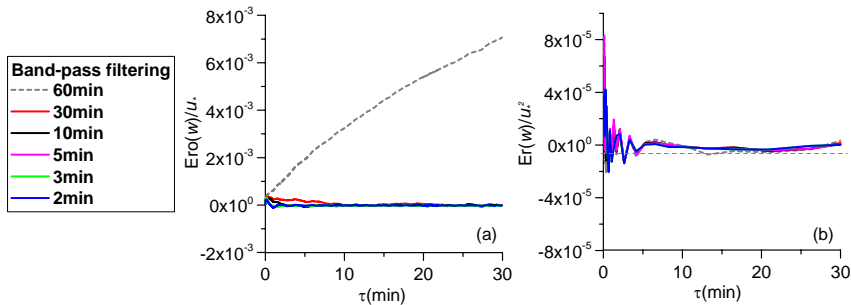


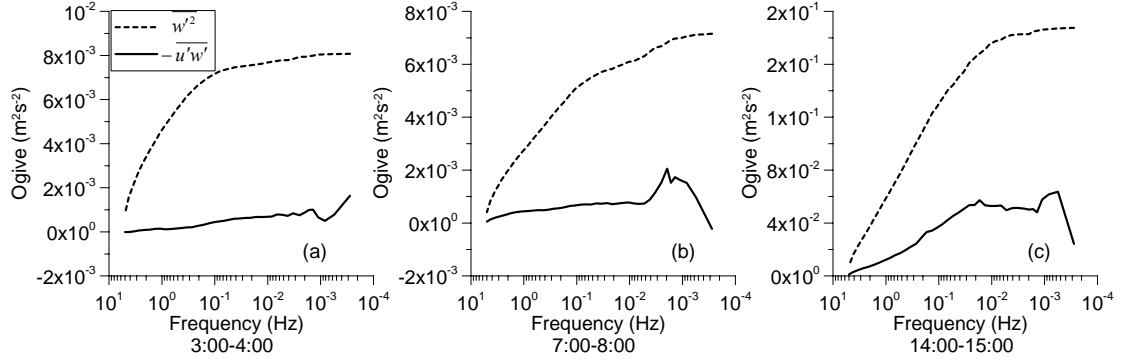
Fig. 6. Variation of mean ergodic function (a) and autocorrelation ergodic function (b) of the vertical velocity with relaxation time for the different scale eddies in the seven stations of CASES-99.

1018

1019

1020

1021

Fig. 7. Variation of Ogive functions of $\overline{w'^2}$ and $-\overline{u'w'}$ with frequency at height 3.08 m for the three time frames in NSPCE.

1027

1028

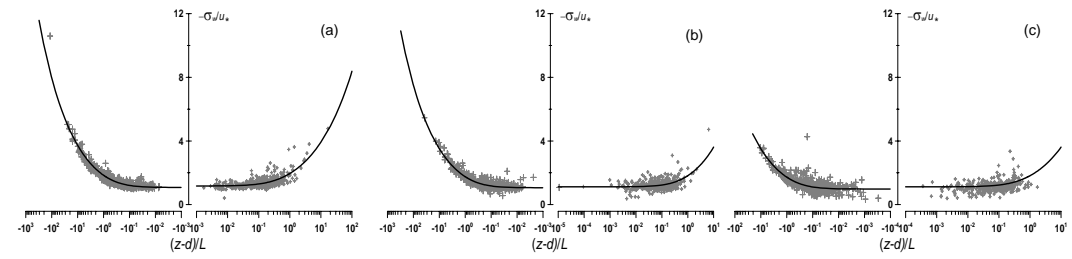


Figure 8. MOS relation of vertical velocity variances of the different scale eddies in NSPCE; Panels (a), (b) and (c) respectively represent the similarity of eddies of 10 min, 30 min and 60 min in the temporal scale.

1034

1036

1037

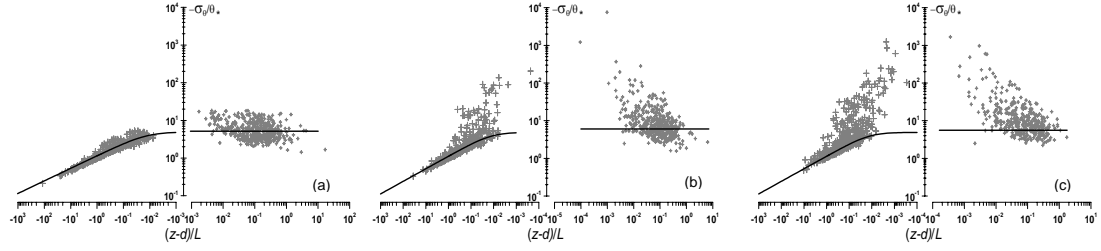


Figure 9. MOS relations of temperature variance of in different scale eddies of NSPCE; Panels (a), (b) and (c) respectively represent the similarity of the eddies of 10 min, 30 min and 60 min in the temporal scale.

1044

1045

1046

1047

1048